

# The muonic hydrogen Lamb shift experiment

R. Pohl<sup>a,b</sup>, A. Antognini<sup>b</sup>, F.D. Amaro<sup>c</sup>, F. Biraben<sup>d</sup>,  
J.M.R. Cardoso<sup>c</sup>, C.A.N. Conde<sup>c</sup>, A. Dax<sup>a,e</sup>, S. Dhawan<sup>e</sup>,  
L.M.P. Fernandes<sup>c</sup>, T.W. Hänsch<sup>b</sup>, F.J. Hartmann<sup>f</sup>,  
V.-W. Hughes<sup>†e</sup>, O. Huot<sup>g</sup>, P. Indelicato<sup>d</sup>, L. Julien<sup>d</sup>,  
P.E. Knowles<sup>g</sup>, F. Kottmann<sup>h</sup>, Y.-W. Liu<sup>i</sup>, L. Ludhova<sup>a,g</sup>,  
C.M.B. Monteiro<sup>c</sup>, F. Mulhauser<sup>g</sup>, F. Nez<sup>d</sup>, P. Rabinowitz<sup>k</sup>,  
J.M.F. dos Santos<sup>c</sup>, L.A. Schaller<sup>g</sup>, C. Schwob<sup>d</sup>,  
D. Taqqu<sup>a</sup>, and J.F.C.A. Veloso<sup>c</sup>

<sup>a</sup>PSI Switzerland, <sup>b</sup>MPQ Garching, Germany, <sup>c</sup>Coimbra Portugal,

<sup>d</sup>LKB Paris, France, <sup>e</sup>Yale USA, <sup>f</sup>TU München, Germany,

<sup>g</sup>Fribourg Switzerland, <sup>h</sup>ETH Switzerland, <sup>i</sup>Hsinchu Taiwan,

<sup>k</sup>Princeton USA

The ongoing experiment to measure the 2S Lamb shift in muonic hydrogen is presented. The aim is to determine the root-mean-square (rms) charge radius of the proton to  $10^{-3}$ , about a factor of 20 times better than presently known from electron scattering experiments or spectroscopy in ordinary hydrogen.

## 1 Introduction

The charge radius of the proton, the simplest nucleus, is known only with a surprisingly low precision of about 2 %. Recent reevaluation of all the electron scattering data [1] yields a value of 0.895(18) fm. The poor knowledge of the proton charge radius restricts tests of bound-state QED to the precision level of about  $6 \times 10^{-6}$ , although the experimental data themselves (Lamb shift in hydrogen) have reached a precision of  $2 \times 10^{-6}$ . The

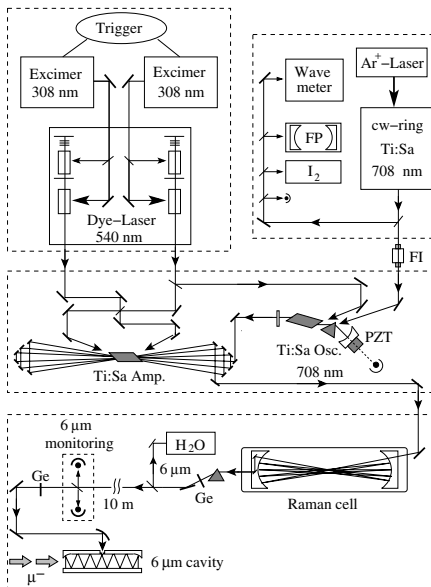


Figure 1: Schematic view of the laser system. The main components are a pulsed excimer-dye laser system, a tunable cw Ti:Sa laser, a pulsed oscillator-amplifier Ti:Sa laser, a Raman cell, and a 6  $\mu\text{m}$  mirror cavity with its diagnostic system. FP: Fabry-Perot, I<sub>2</sub>: iodine absorption cell, H<sub>2</sub>O: water absorption cell, PZT: piezo transducer, FI: Faraday Isolator.

determination of the proton charge radius with an accuracy of  $10^{-3}$  is the main goal of our collaboration. This level of precision opens the way to check bound state QED predictions towards a level of  $10^{-7}$  precision [2, 3].

Our  $\mu\text{p}$  Lamb shift experiment will measure the energy difference between the  $2^3\text{S}_{1/2} - 2^5\text{P}_{3/2}$  atomic levels in muonic hydrogen to a precision of 30 ppm, i.e. 10 % of the natural line width. Very low-energy negative muons are stopped in 0.6 mbar of hydrogen gas, where, following the  $\mu^-$  atomic capture and cascade, 1 % of the muonic hydrogen atoms form the metastable  $2\text{S}$  state with a lifetime of  $1.3\ \mu\text{s}$ . A  $6\ \mu\text{m}$  laser pulse is used to drive the  $2\text{S} \rightarrow 2\text{P}$  transition. On resonance, quasi instantaneous deexcitation to the  $1\text{S}$  state takes place, and the emitted 1.9 keV x ray is detected by Large Area Avalanche Photodiodes (LAAPDs). The resonance frequency, and hence the Lamb shift and the proton charge radius, is determined by measuring the intensity of the x-ray fluorescence as a function of the laser wavelength.

During the latest measurement period (July–December 2003) a broad range of laser frequencies was scanned, but no signal of a resonance was found. Improvements on the laser system are currently under way.

## 2 Experiment

The experimental setup is described in detail elsewhere [4]. In summary, about  $320\text{ s}^{-1}$  low energy  $\mu^-$  (3-6 keV kinetic energy) are detected by the muon entrance detectors and enter the gas target filled with 0.6 hPa  $\text{H}_2$  gas. An anticoincidence detector at the end of

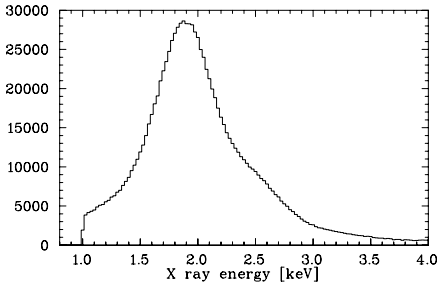


Figure 2: X-ray energy spectrum measured at 0.6 hPa  $\text{H}_2$  pressure. Summing the laser ON and laser OFF data from all 20 LAAPDs gives  $1.07 \times 10^6$  events.

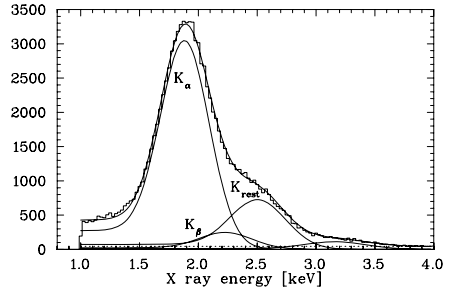


Figure 3: X-ray energy spectrum of *one* LAAPD and the fitted  $K_\alpha$ ,  $K_\beta$  and  $K_{\text{rest}}$  lines (plus a weak line at 3.1 keV).

the gas target rejects muons that did not stop. This results in  $240 \text{ s}^{-1} 12\bar{3}$  signals which can trigger the laser system. The intrinsic dead time of our laser system (until now given by the excimer and dye lasers) limits the number of “events with laser” to approx.  $60 \text{ s}^{-1}$ .

The laser system used in 2003 is shown in Fig. 1. The main requirement of the whole system is that the time difference between a trigger pulse (given by a muon arriving *at random times*) and the light output has to be of the order of the *lifetime of the  $\mu\text{p}(2\text{S})$  state*, i.e.  $\sim 1.5 \mu\text{s}$ .

Two XeCl excimer lasers provide enough energy ( $\sim 650 \text{ mJ}$  total) with a reasonable short internal delay of  $\sim 1 \mu\text{s}$ . The 308 nm light is used to pump two dye lasers (each oscillator plus amplifier) delivering  $\sim 100 \text{ mJ}$  at 540 nm.

This green light pumps a Ti:sapphire oscillator-amplifier system lasing at 708 nm. This red light is injected into a high-pressure  $\text{H}_2$  Raman cell where three sequential Stokes shifts convert the 708 nm light to the desired  $6 \mu\text{m}$  laser light required to drive the  $\mu\text{p}(2\text{S}-2\text{P})$  transition. We obtain approximately  $0.2 \text{ mJ}$  per pulse at  $6 \mu\text{m}$ . The IR light is then injected into a multipass cavity surrounding the muon stop volume inside the hydrogen target.

The pulsed Ti:Sa oscillator is injection-seeded by a tunable cw Ti:Sa laser. The IR wavelength is scanned by changing the wavelength of the cw Ti:Sa seed laser. The cw Ti:Sa laser is locked to a very stable Fabry-Perot (FP) interferometer with a mode spacing of  $1.5 \text{ GHz}$ .

On resonance the laser-induced  $2\text{S} \rightarrow 2\text{P}$  transition is quasi instantaneously followed by a  $2\text{P} \rightarrow 1\text{S}$  transition to the ground state. The  $1.9 \text{ keV}$  muonic  $K_\alpha$  x-ray emitted therein is recorded in large area avalanche photodiodes (LAAPDs), 20 of which are mounted as close as 8 mm away from the muon beam axis. The LAAPD energy and time resolution are typically  $\Delta E/E \approx 25 \%$  (FWHM) and  $\Delta t \approx 35 \text{ ns}$  for  $2 \text{ keV}$  x-rays. An energy cut around  $2 \text{ keV}$  is used to reduce the background significantly. Additional background reduction is achieved by requesting a signal from the electron originating from the muon decay, after a  $2 \text{ keV}$  x-ray has been seen. These muon decay electrons are either seen in

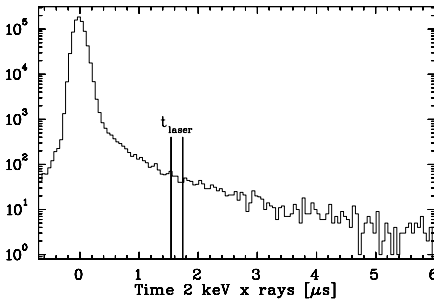


Figure 4: Time spectrum of 2 keV x-rays, summed from laser OFF and all laser ON runs at all wavelengths. The laser time window is indicated.

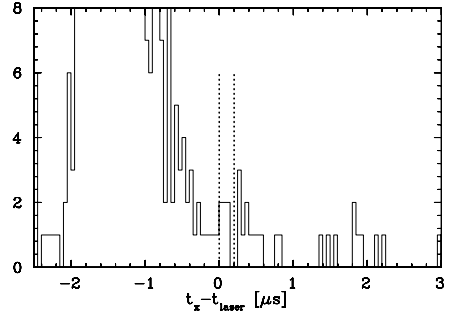


Figure 5: Laser-time corrected time spectrum of the laser ON events for one laser wavelength (“FP 843”). 6 events are seen in the laser time window 0...200 ns (dotted lines). The number of prompt events at (-2...-1  $\mu$ s) is  $2.1 \times 10^4$ .

the LAAPDs, or in one of five scintillators read out by photomultiplier tubes.

### 3 Results

More than  $10^6$  x-rays from  $\mu$ p K-line transitions ( $K_\alpha$ ,  $K_\beta$ , and  $K_{\text{rest}}$ , at 1.895, 2.246, and  $\sim 2.44$  keV, respectively) were recorded at 0.6 hPa  $\text{H}_2$  ( $T=300$  K). This is at least two orders of magnitude more than in any previous muonic hydrogen measurement performed at such low gas densities. The laser was fired for  $\sim 30\%$  of the events (“laser ON” events). Additional “laser OFF” events were recorded between two laser shots, during the dead time of the laser, to determine the background with optimum statistics.

The measured x-ray energy spectrum, summed up for all LAAPDs, and laser ON and OFF events, is shown in Fig. 2. This summed spectrum cannot be fitted with a simple sum of Gaussians, because the different LAAPDs have different energy resolutions. Figure 3 gives an example of the data obtained in *one* LAAPD, together with the fit.

Figure 4 shows the time spectrum of all good data (laser ON and laser OFF) taken during the 16 days of data taking in the end of 2003. The prompt peak at time 0 originates from  $\mu$ p atoms that do not form metastable  $\mu$ p(2S) atoms, but deexcite to the  $\mu$ p(1S) ground state thereby emitting a muonic K-x-ray. The delayed background seen in Fig. 4 originates mainly from muonic carbon x-rays:  $\mu$ p(1S) atoms arriving at the target walls transfer the muon to the carbon which results in 5 keV x-rays. These can show up as 2 keV x-rays in the LAAPDs, because the 5 keV peak has a significant tail towards lower energies.

One cannot expect to see a signal in Fig. 4, because it contains laser OFF events and all laser ON events at all wavelengths, but the plot is interesting because it shows the very low

background level reached: 215 background events in the laser time window  $1.52 \dots 1.72 \mu\text{s}$  for  $7.8 \times 10^5$  prompt events, i.e.  $2.8 \times 10^{-4}$  delayed/prompt. With currently approx. 2000 prompt events per hour with laser ON, this corresponds to a background rate of 0.6 background events per hour.

Figure 5 shows the laser ON time spectrum for *one* FP fringe, i.e. for one laser wavelength. Each event in this time spectrum has been corrected for the true arrival time of the laser puls in the target cavity, so the laser-induced events are expected in the time window  $0 \dots 200$  ns (due to the light confinement time of the laser cavity of  $\sim 145$  ns).

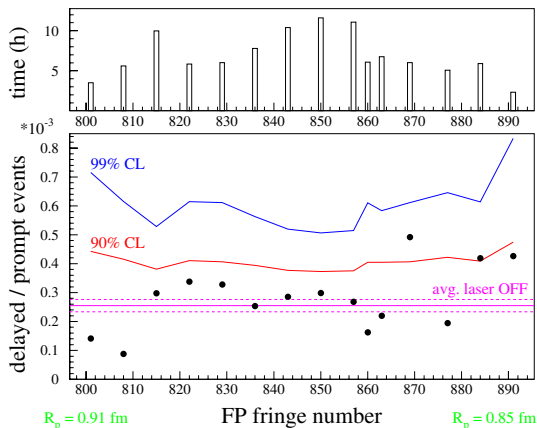


Figure 6: Results of the 2003 run. Black dots are the number of delayed events in the laser time window normalized to the number of prompt events. The FP fringe number is a measure for the laser wavelength. The confidence levels are for the hypothesis “only background”. The upper plot shows the approximate measuring time per point.

The final result of the 2003 run is shown in Fig. 6. For each wavelength (shown in units of the FP fringe number) we plotted the number of delayed events in the laser time window divided by the number of prompt events, thereby normalizing to the true number of useful laser shots at this wavelength. The expected number of background events is shown as the “avg. laser OFF” line, and the lines “90% CL” and “99% CL” indicate the 90 and 99% confidence levels for the hypothesis “data contains only background”. The top graph shows the approximate measurement time per point.

No resonance is seen in Fig. 6, but the statistics is so low that we can also not exclude that the RMS proton charge radius is in the interval  $0.85 \dots 0.91$  fm.

## 4 Outlook

The experience from the run 2003 is that the basic concepts of muon beam, x-ray detectors and laser system are sound and that the apparatus worked reliably. However, the event

rate is obviously too small. We are therefore now working on improvements which should increase the event rate by more than a factor of 30.

The main improvement will come from replacing the excimer and dye lasers, which are responsible for the long delay and the low repetition rate, by a so-called “disk-laser” [5]. This is a cw-pumped Ytterbium:YAG laser disk which does not suffer from thermal lensing due to its geometry. The 1030 nm light of this laser will be frequency-doubled and this green laser light will then be used to pump the Ti:Sa lasers.

Tests have shown that the intrinsic delay of the disk laser is only a few hundred nanoseconds, and the repetition rate can be as high as a few hundred Hertz.

We are confident that the expected improvements will lead to a successful experiment in 2006.

## References

- [1] I. Sick, Phys. Lett. B **576**, 62 (2003).
- [2] M. Niering *et al.*, Phys. Rev. Lett. **84**, 3232 (2000).
- [3] B. de Beauvoir *et al.*, Eur. Phys. J. D **12**, 61 (2000).
- [4] R. Pohl *et al.*, Can. J. Phys. **83**, 339 (2005).
- [5] Ch. Stewen *et. al.*, IEEE J. of Selected Topics in Quant. Electr. **6**, 650 (2000).